ADVANCED SUSTAINABLE SYSTEMS
www.advsustainsys.com

# Marine Fouling Characteristics of Biocomposites in a Coral Reef Ecosystem

*Marco Contardi,* Simone Montano,* Paolo Galli, Giulia Mazzon, Amin Mah'd Moh'd Ayyoub, Davide Seveso, Francesco Saliu, Davide Maggioni, Athanassia Athanassiou,* and Ilker S. Bayer*

**Coral reefs are among the most diverse ecosystems in the world. The diversity of life found in the habitats created by corals is so large that the reefs are known as the "rainforests of the sea." Unfortunately, severe natural and anthropogenic changes such as ocean warming, acidification, coral diseases, and plastic pollution are extremely detrimental to this ecosystem. To enrich the ambient conditions of the corals and boost their growth, the potential of two biocomposites is evaluated based on biodegradable polyurethane and silicone matrices as scaffolds for the growth of oceanic organisms. Furthermore, their degradation is investigated within the coral reefs of Faafu Atoll, Republic of Maldives. The observations indicate that there are a significant number of organisms that settle and grow on these biocomposites in the Maldivian lagoon, both of an animal and photosynthetic nature. The biocomposites have the potential to become suitable scaffolds for diverse hard bottom fouling organisms. Moreover, the presence of coral larvae on the biocomposites suggests that during their biodegradation, these biocomposites can support the growth of organisms, generating a suitable environment for triggering the birth of new corals.**

## 1. Introduction

Coral reefs are undergoing both human-related and natural stressors that are dramatically jeopardizing this ecosystem. Indeed, they are facing threats at varying temporal and spatial scales such as climate change, overfishing, ocean warming and acidification, diseases, and pollution.[1] Moreover, micro and macro plastics have been highlighted as a new emergent threat to coral reefs.[2] These objects can float in the sea for years and affect the life quality of the organisms that live in this fragile ecosystem in many multiple ways.[3] In a recent study, for example, Lamb et al.[4] demonstrated a strict correlation between the presence of plastic in the sea and the increased outbreak of coral diseases, suggesting that plastic pieces can act as a vector for pathogens. Furthermore, coral reefs are not only a meaningful resource of biodiversity, since they are the most diverse marine ecosystem of the world, but also a socio-economical support for 275 million people.[5] For these reasons, the development of mitigation and restoration techniques for corals is gaining attention in the scientific communities.[6]

Biodegradable bioplastics are emerging as an alternative to the common recalcitrant oil-derived plastics to reduce the end-of-life related green house gas (GHG) emission, and accelerate their natural degradation rate, making them eco-friendly and sustainable. Several strategies have been proposed for the design of efficient and scalable biodegradable plastics, from the synthesis of biodegradable polymers derived either from renewable feedstock[7] or from oils[8] to the direct employment of natural polymers[9] or composite-modified organic agro-wastes,[10] keeping the excellent properties of the common plastics. In this work, since we were investigating the use of bioplastics as scaffolds for the growth of corals in the marine environment we focused on biodegradable plastics but with prolonged degradation times.

Polyurethane (PU) is one of the most widely used plastic materials and is mostly utilized for surface coatings, foams, electronic components, adhesives, sealants, carpets, and food packaging. Biodegradation of PU is a slow process involving water, acid, alkaline or oxidative conditions.[11] In addition, PU-based materials can be digested by enzymatic reactions mediated by microorganisms that release lipase, urease, protease, and esterase.[12] Indeed, in the early 2000s, scientists discovered that *Pseudomonas* strains could release specific enzymes able to degrade PU.[13] From that moment, several microorganisms, both bacteria and fungi, have been found capable of degrading PU and probably consuming it as a source of carbon and nitrogen.[12b]

Dr. M. Contardi, Dr. G. Mazzon, A. Mah'd Moh'd Ayyoub, Dr. A. Athanassiou, Dr. I. S. Bayer
Smart Materials
Istituto Italiano di Tecnologia
Genova 16163, Italy
E-mail: marco.contardi@iit.it; athanassia.athanassiou@iit.it

Dr. S. Montano, Prof. P. Galli, Dr. D. Seveso, Dr. F. Saliu, Dr. D. Maggioni
Department of Earth and Environmental Sciences (DISAT)
University of Milan, Bicocca
Milan 20126, Italy
E-mail: simone.montano@unimib.it

Dr. S. Montano, Prof. P. Galli, Dr. D. Seveso, Dr. F. Saliu, Dr. D. Maggioni
MaRHE Center (Marine Research and High Education Center)
Magoodhoo Island, Faafu Atoll, Malé 12030, Republic of Maldives

The ORCID identification number(s) for the author(s) of this article can be found under https://doi.org/10.1002/adsu.202100089.



**DOI: 10.1002/adsu.202100089**

Biodegradation of PU has also been investigated in different environments. Various fungal communities in the soil are able to interact with the synthetic polymers and grow on their surfaces.[14] Specifically for the sea environment that is of interest for this work, Davies and Evrard[15] tested soft and rigid PU in the sea of Brest in France for 5 years. The authors revealed initial hydrolysis of the material's surface by infrared spectroscopy, but the overall mechanical properties of the polymers were not affected, suggesting a long-term degradation and proving the suitability of these materials for long-term underwater applications. In addition, Rutkowska et al.[16] tested PU in the Baltic Sea for 12 months and demonstrated a direct dependence between the crosslinking degree and the degradation rate.

Nonetheless, PU is still considered as part of plastic pollution in the seas. However, several efforts have been made to produce more eco-friendly PU polymers. For instance, Wondu et al.[17] recently described the polymerization of a fully water-soluble PU based on polyethylene glycol. Several polyester-based PUs have been made from polycaprolactone diols that can easily hydrolyze even in neutral pH waters.[18] In many waterborne PU dispersions, in addition to polycaprolactone diols (soft segments), an isophorone diisocyanate is used to form the hard segments, allowing their use in many medical applications as well.[19] Moreover, new generation biodegradable PU dispersions in water having polycaprolactone–polyethylene glycol copolymer soft segments have also been reported recently with tunable mechanical properties.[20] Although the biodegradable segments still originate from petroleum-based monomers and precursors, the final resins have been shown to be nontoxic and easily hydrolyzed even in the absence of microbial activity. To further ensure the biodegradation of the developed materials, in this work PU was used in combination with lecithin and wax.

Similarly, silicone is an elastomeric polymer widely utilized in different fields, from medicine to antifouling coatings. Polydimethylsiloxane (PDMS) is an attractive polymer for long-lasting applications, but at the same time, able to be degraded if accidentally dispersed in the environment. Indeed, in 1994, Lehmann et al. evaluated in several studies the degradation of PDMS, showing how the environment can metabolize it into $CO_2$.[21] In addition, other studies described how PDMS is quickly hydrolyzed in the soil in its water-soluble monomer dimethylsilanediol.[22] Finally, Sabourin et al.[23] discovered that some bacteria and fungi species could co-metabolize the PDMS monomer to $CO_2$, demonstrating the PDMS biodegradability. In recent studies, our group evaluated silicone as potential material for the production of bioplastics combining it with natural materials such as starch, cocoa shell waste, and red beetroot to improve its antioxidant and barrier properties.[24] In addition, the developed bioplastics showed an encouraging degradation rate in the biochemical oxygen demand (BOD) tests. In this work PDMS was used in combination with starch in a ratio PDMS/starch 40:60. The integration of starch into plastics manufacturing has resulted in lower consumption of nonrenewable energy resources (50%) and, therefore, less greenhouse gas emissions (60%) compared to the polystyrene (PS) packaging.[25]

An innovative strategy to enrich the coral reef ecosystem could be the design and development of biocomposites that can create a sustainable environment for marine organisms, either when placed on purpose, or if accidentally dispersed in the sea. For this reason, evaluating potential interactions between marine ecosystem and biocomposites during their prolonged degradation can be a stimulating point for selecting potential new tools in order to support coral reef recovery. Motivated by these prospects in this study, the two biocomposites mentioned above were fabricated and characterized in terms of morphology, chemical, mechanical, and water interaction properties. In particular, one was based on a biodegradable PU–wax–lecithin waterborne emulsion and the other was based on a single component silicone resin and corn starch. The degradation of the two biocomposites was evaluated by placing them underwater in the Maldives Sea for 6 months. After this period, the presence of marine organisms on the surface biocomposites was also assessed.

## 2. Results and Discussion

### 2.1. Preparation of the Biocomposites and Morphological Analysis

The two biocomposites were produced following different procedures. The starch–PDMS-based composite was made by dispersing the PDMS in hepthane and mixing it with starch particles at a weight ratio of 40:60. After mixing and homogenizing, the sample was dried for 4 days under an aspirated hood (16–20 °C and 40–50% RH). This preparation has been extensively described in our previous work.[24a] Further details are reported in the Experimental Section. The preparation of lecithin/wax/polyurethane-based (LWPU) samples is schematically shown in the **Scheme 1** and started by dissolving lecithin pellets in water by using a sonicator. Upon dispersion of all the soy lecithin, wax pellets were added. The mix was warmed in order to promote melting of the wax and then sonicated. At this point, the solution appears milky and stable. Afterward, the PU dispersion was added to the milky emulsion and sonicated again. Upon homogenization, the films could be cast directly in molds.

Photographs of the produced LWPU and starch–PDMS biocomposites are shown in **Figure 1**A,B, respectively, while in Figure S1A,B in the Supporting Information, photographs of pristine PU and PDMS are reported.

The water-based PU suspension after the solvent evaporation resulted in being a transparent, colorless material (Figure S1A, Supporting Information). Instead, the LWPU biocomposite showed a slight yellowish color, as can be noticed in Figure 1A, while no macroscopic phase separations were observed. Starch–PDMS biocomposites formed white materials (Figure 1B), while PDMS was totally transparent and colorless (Figure S1B, Supporting Information).

In Figure 1C–H; Figure S2C–F in the Supporting Information, scanning electron microscopy (SEM) images acquired from the top-view and the cross-sections of the biocomposites and the pristine polymers PU and PDMS are displayed. Figure 1C shows the top-view of LWPU sample prepared by the emulsion method. The surface of LWPU resulted in being flat, but some roughness can be noticed. The cross-section highlighted the dispersion of wax microdrops in the polyurethane

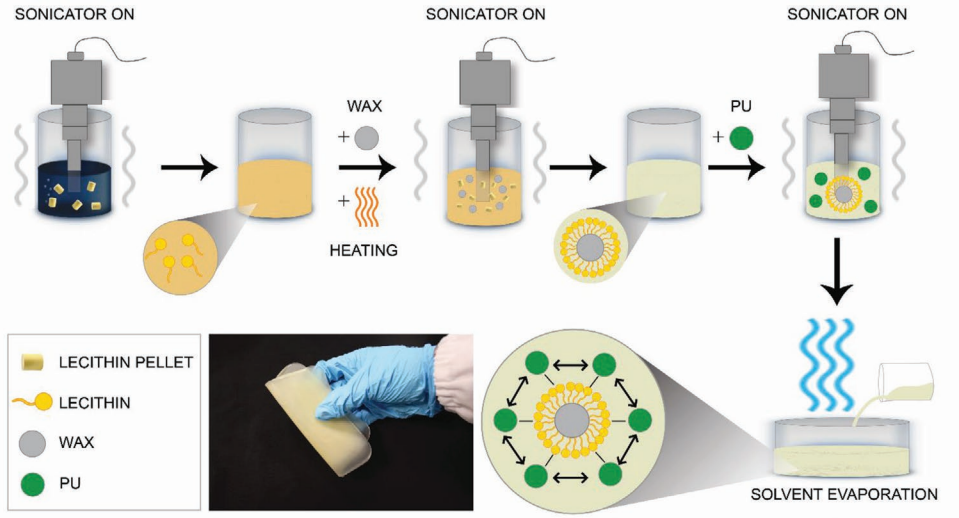


**Scheme 1.** Schematic representation of the LWPU biocomposite production and the different assembly in the final material with respect to the pristine PU.

matrix, suggesting a well-assembled solid emulsion, as can be noted in Figure 1E and highlighted by the red arrows in Figure 1G. The morphological change can also be confirmed by the comparison of the cross-section of LWPU with the pure PU, reported in Figure S2E in the Supporting Information, the cross surface of the second being very smooth. Therefore, in the pristine sample, the particles of PU suspended in water, during the solvent evaporation, interact with each other, assembling in a well-defined compact and ordered structure, also confirmed by the transparency of the sample (Figure S2A, Supporting Information). On the other hand, when lecithin and wax are presented in the solution, the assembly process most probably changes and the final structure resulted in being modified, as we schematically represent in Scheme 1.

Both the surface and the cross-section of the starch–PMDS samples were characterized by the visible presence of starch granules entrapped in the PDMS material, as can be noticed in Figure 1D, F and highlighted by the red arrows in Figure 1H. The pristine PDMS material showed a smooth surface and cross-section, as can be observed in Figure S2B,D,F in the Supporting Information.

### 2.2. Chemical Analysis

The two biocomposites were chemically characterized using attenuated total reflection–Fourier transform infrared ATR–FTIR. In **Figure 2**, the spectrum of soybean lecithin shows the typical vibrational modes of the natural emulsified agent: asymmetric and symmetric $CH_3$ stretching modes at 2955 and 2872 $cm^{-1}$, respectively, asymmetric and symmetric $CH_2$ stretching modes at 2922 and 2853 $cm^{-1}$, respectively, C=O stretching mode at 1736 $cm^{-1}$, C=C stretching modes at 1655 and 1618 $cm^{-1}$, symmetric $CH_2$ scissoring vibrational mode at 1464 $cm^{-1}$, asymmetric and symmetric $CH_3$ scissoring vibrational mode at 1458 and 1377 $cm^{-1}$, respectively, asymmetric and symmetric $PO_2$ stretching mode at 1225 and 1086 $cm^{-1}$, symmetric P–O–C stretching mode at 1049 $cm^{-1}$, and $CH_2$ rocking mode at 719 $cm^{-1}$.

Wax showed typical peaks of an aliphatic compound: asymmetric and symmetric $CH_3$ stretching modes at 2955 and 2872 $cm^{-1}$, respectively, asymmetric and symmetric $CH_2$ stretching modes at 2916 and 2849 $cm^{-1}$, respectively, symmetric $CH_2$ scissoring vibrational mode at 1472 $cm^{-1}$, asymmetric and symmetric $CH_3$ scissoring vibrational mode at 1462 and 1377 $cm^{-1}$, respectively, C—H rocking modes at 889, 729, and 719 $cm^{-1}$.

Instead, for PU, we observed the typical peaks of the polymer: N—H stretching mode at 3331 $cm^{-1}$, C—H stretching modes between 2965 and 2859 $cm^{-1}$, C=O stretching mode at 1728 $cm^{-1}$, O=C—N stretching modes (Amides I and II) at 1695 and 1643, C=C stretching mode at 1545 $cm^{-1}$, C—N stretching mode at 1432 $cm^{-1}$, and C—O—C stretching mode at 1097 $cm^{-1}$.

LWPU spectrum, reported in the bottom part of Figure 2A, showed a good overlap of the main peaks of the three components. Highly intense and narrow peaks in the regions of C—H stretching (2960–2850 $cm^{-1}$), binding (1500–1350 $cm^{-1}$), and rocking modes (800–700 $cm^{-1}$) can be associated with the wax material. Amides, C=C and C=O stretching modes typical of PU can also be noticed. Instead, lecithin peaks were highly merged and covered by the polymer signals. For this reason, PU spectrum was subtracted to the LWPU one and lecithin peaks appeared. Interestingly, a shift in the C=O stretching mode of the lecithin was observed, moving from 1736 to 1744 $cm^{-1}$. Also, the asymmetric and symmetric $PO_2$ stretching modes shifted to 1211 and 1067 $cm^{-1}$, respectively. Shifts in this region were previously described for lecithin involved in H-bonds.[26]

The ATR–FTIR spectrum of the starch-based biocomposite is reported in Figure 2C. Typical signals associated with starch and PDMS were found. Starch: O—H stretching mode at 3331 $cm^{-1}$ and C—O stretching mode at 1150 $cm^{-1}$. PDMS: asymmetric and symmetric $CH_3$ stretching modes at 2965 and 2907 $cm^{-1}$, respectively: symmetric and asymmetric Si–O–Si stretching modes at 1069 and 1005 $cm^{-1}$, respectively; $CH_3$ rocking mode 787 $cm^{-1}$. Interactions between silicone and starch have been previously discussed and described in Ceseracciu et al.[24a]

The physical state of the materials was also investigated by X-ray diffraction (XRD) analysis and the patterns are reported

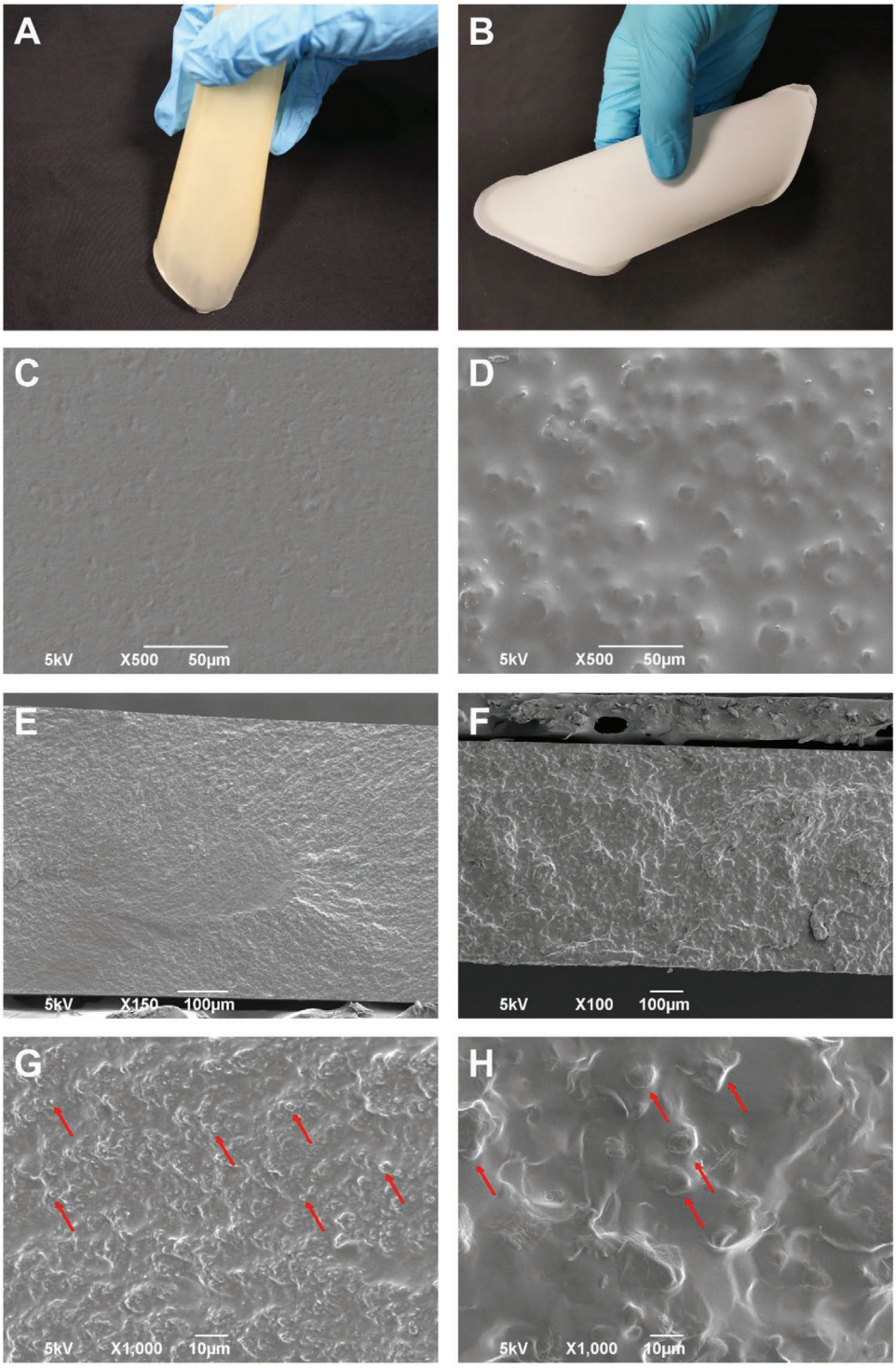


**Figure 1.** A,B) Photograph of LWPU and starch–PDMS biocomposites, respectively. SEM images of C) top-view and E,G) cross-section of LWPU sample. SEM images of D) top-view and F,H) cross-section of starch–PDMS biocomposite. The red arrows highlight the microdrops of lecithin-wax dispersed in the PU matrix of G) LWPU and the starch granules dispersed in the H) PDMS.

in Figure S3A,B in the Supporting Information. Specifically, PU showed a broad peak centered at 18.5° $2\theta$, typical of amorphous soft PU,[27] while lecithin had the characteristic broad peak centered at 20.0° $2\theta$ typical of its amorphous state,[28] and wax presented two peaks at 21.5° and 23.9° $2\theta$.[29] Instead, when these compounds were combined together in the LWPU samples, three main peaks at 19.2°, 21.6°, and 24.0° could be observed and assigned to PU/lecithin, the first one, and wax, the other two. Therefore, lecithin and PU maintained their amorphous state while wax kept its crystalline nature in the final mix.

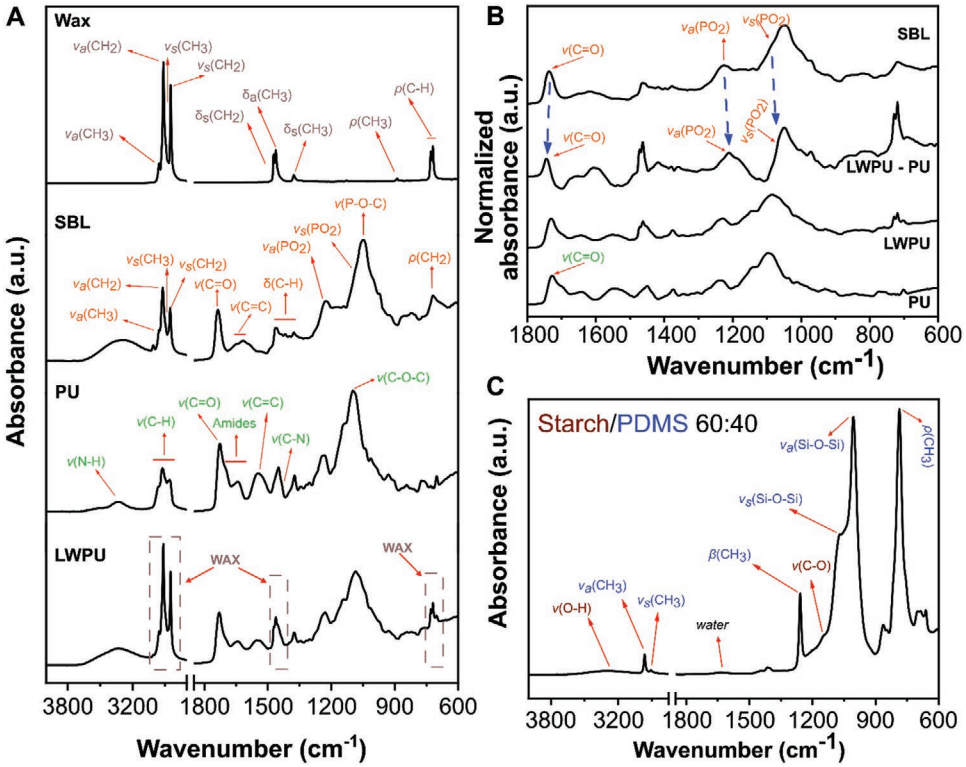


**Figure 2.** A) ATR–FTIR spectra of wax, soybean lecithin, polyurethane, and LWPU samples. B) Comparison in the spectral region of 1800–600 $cm^{-1}$ of soybean lecithin, subtracted spectrum LWPU–PU, LWPU, and PU. C) ATR–FTIR spectrum of starch/PDMS sample.

The most significant peaks of the typical crystalline structure of starch were found at 11.7°, 15.1°, 17.3°, 18.1°, 23.0°[30] while PDMS was in an amorphous condition and presented two broad peaks at 11.9° and 21.8°. In the starch/PDMS, overlapped peaks were found, in particular at 11.9° (from both PDMS and starch), 15.1° (from starch), 17.1° (from starch), 18.1° (from starch), and 23.2° (from starch).

### 2.3. Thermal Characterization

Thermal properties of the biocomposites and their pristine components were evaluated, and the results are reported in Figure S4A,B in the Supporting Information. In Figure S4A in the Supporting Information, the thermograms and derivative thermogravimetric curves of lecithin, wax, PU, and LWPU are shown. Lecithin thermal decomposition presented several events in a wide range of temperatures. In particular, the first event at 130 °C was probably connected with residual humidity evaporation. Afterward, events at 186, 200, 265, 333, 364, 425, and a tiny one at 526 °C were observed.[31] Instead, wax resulted in being thermally stable until high temperature. Indeed, two main events of decomposition occurred for the wax sample at 295 and 386 °C.[32] PU showed three thermal events at 312, 395, and 453 °C.[27] Finally, LWPU showed decomposition for a broader range of temperature. Indeed, the degradation started around 160 °C, and then a higher quantity of weight loss was registered in this initial phase, mainly due to the presence of wax and lecithin and completing in a first maximum at 280 °C. After that, two main events were found at 329 and 403 °C while for PU were at 312 and 395 °C. The total decomposition was also shifted with respect to the pristine polymer from 476 to 500 °C. Therefore, in the LWPU samples, these differences with the changes in the FTIR spectra and in the morphology could suggest that lecithin emulsify the wax with its aliphatic chains while its polar head is exposed to the water environment, further, while the evaporation solvent occurs, this latter interacts with the hydrophilic part of the PU generating different assembly respect to the pristine polymeric material as schematically shown in Scheme 1.

In the thermogram of starch, the first loss of weight was noticed at 51 °C due to environmental humidity that interacts with the O—H groups of the polysaccharide,[33] then a unique event of decomposition was observed at 311 °C. PDMS was characterized by two thermal events at 536 and 653 °C. Instead, in the starch/PDMS samples, the starch decomposition occurred at 297 °C, and the events connected with the silicone material are shifted at 515 and 599 °C, suggesting that strong interactions of the two polymers occur when combined together.[24a]

### 2.4. Mechanical Properties

The mechanical properties of biocomposites were investigated and compared to pristine PU and PDMS, and the results are reported in **Figure 3**. Stress–strain curves of PU, LWPU, starch/PDMS, and PDMS samples are shown in Figure 3A. The values of Young's Modulus (YM) and stress at maximum load (STM) of the samples are reported in Figure 3B. In detail, the pristine

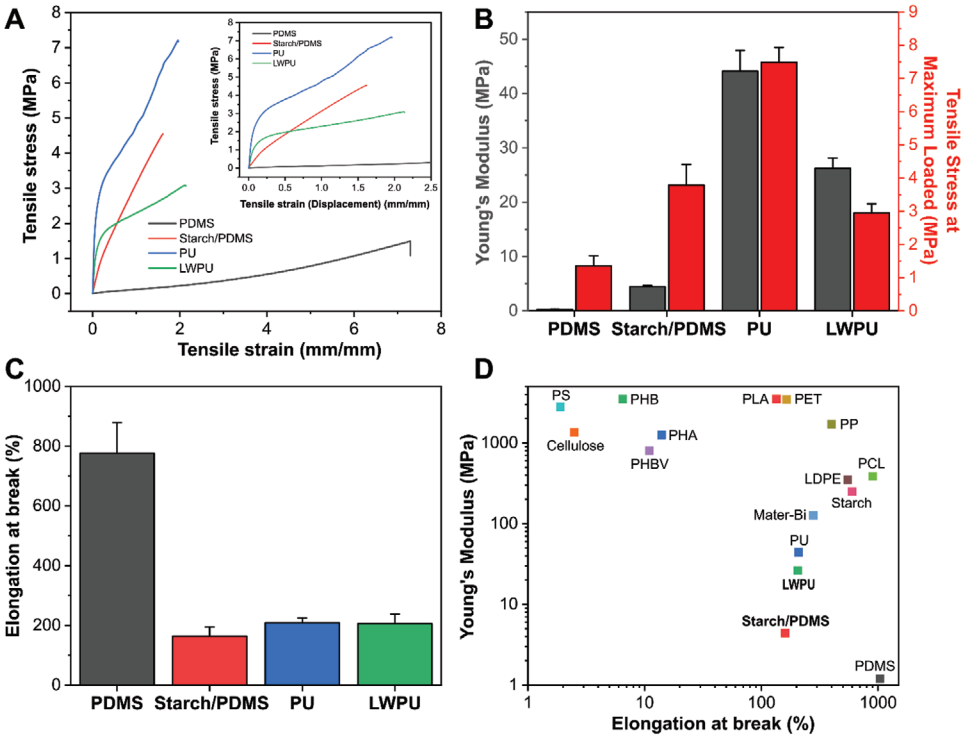


**Figure 3.** A) Stress–strain curves of PMDS, starch/PDMS, PU and LWPU biocomposites. The insert displays the curves at lower stain values. B) Values of Young's Modulus and tensile stress at maximum load of PDMS, starch/PDMS, PU and LWPU samples. C) Percentage of elongation at break of PDMS, starch/PDMS, PU, and LWPU materials. D, Plot of elongation at break versus Young's Modulus values for various polymeric commercial plastics as a comparison to the LWPU and starch/PDMS described in this study.

PU material had YM and STM of 44.1 ± 3.8 and 7.5 ± 0.4 MPa, respectively, while LWPU showed an YM of 26.2 ± 1.9 MPa and an STM of 2.9 ± 0.3 MPa. The elongation at break of the PU and LWPU samples were 209.0 ± 15.4% and 205.7 ± 31.1% and the results are displayed in Figure 3C. These differences suggested that lecithin and wax act as plasticizer/softener of PU, reducing by 50% the YM and STM but keeping in the same range the elongation capacity.

PDMS is an elastomer material and has an YM of 0.28 ± 0.04 MPa, a STM 1.35 ± 0.3 MPa, and an elongation at break of 776.4 ± 102.0%. Instead, when starch is introduced in the polymeric structure, the elongation at break is reduced at 160%, while the YM and STM are 4.4 and 3.8 MPa. This change in the mechanical properties of the filled PDMS material was not unexpected. Indeed, in our previous work,[24a] we described how the introduction of starch granules can modify the elastomeric behavior of the siloxane to a linear elastic profile, making it a more robust material.

Finally, the YM and the elongation at break of the two soft and ductile biocomposites were compared with other petroleum-based plastics and biopolymers such as PS,[34] polyethylene terephthalate (PET)[34] polypropylene (PP),[34] low-density polyethylene (LDPE),[34] polyhydroxyalkanoate (PHA),[34] polyhydroxybutyrate (PHB),[34] poly(3-hydroxybutyrate-*co*-3-hydroxyvalerate) (PHBV),[34] polycaprolactone (PCL),[35] polylactic acid (PLA),[34] cellulose,[36] starch, and Mater-bi.[37]

As can be noticed in Figure 3D, the LWPU and starch–PDMS showed comparable mechanical properties to the common polymers and plastics used for food packaging or plastic bag production, suggesting their potential employment for various fields of application.

### 2.5. Wettability, Water Vapor Permeability, and Water Uptake Properties

Before immersing the biocomposites in the marine environment, the interactions between water and the biocomposites were thoroughly investigated.

The results of wettability, water vapor permeability, and water uptake are presented in **Figure 4**. Static water contact angle (WCA) of PDMS, starch/PDMS, PU, and LWPU was evaluated, and the results are shown in Figure 4A. PDMS is a well-known hydrophobic compound and had a WCA of 120°. Similar contact angle was observed for the starch-based biocomposite (121°), indicating that the introduction of starch granules inside the silicone matrix did not affect the final surface behavior.

PU showed a WCA of ≈75°, while when the lecithin and wax were added into the polymeric structure, the surface of the material became more hydrophilic, having a WCA of ≈ 24°. The increased hydrophilicity can be explained by the exposition of the polar head of the lecithin on the material's surface, while the wax material is protected inside the emulsion and is not exposed. Similar behavior was also noticed by Nirmala et al.[38] when lecithin was introduced in polyamide-based nanofibers.

Barrier properties of PDMS, starch/PDMS, PU, and LWPU were investigated by calculating the water vapor transmission rate and the water vapor permeability value, following the

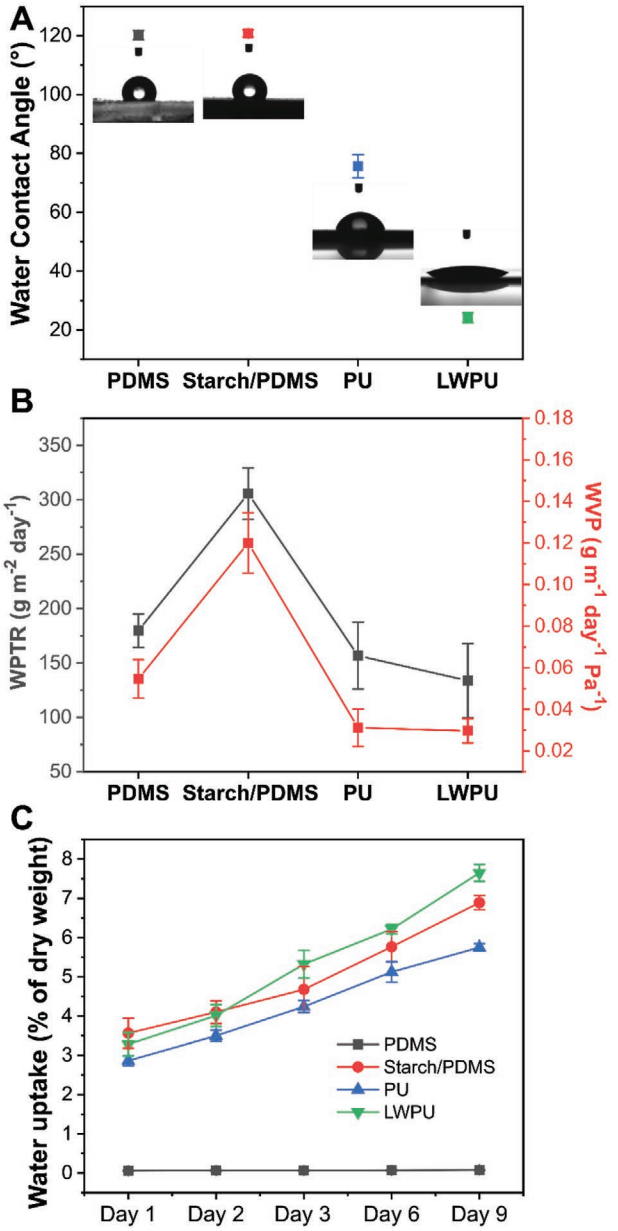


**Figure 4.** A) Water contact angle of PDMS, starch/PDMS, PU, and LWPU samples. B) Water vapor transmission rate (WVTR, gray color) and water vapor permeability (WVP, red color) of PDMS, starch/PDMS, PU and LWPU samples. C) Water uptake capacity of PDMS, starch/PDMS, PU and LWPU samples at 100% R.H. condition after 1, 2, 3, 6, and 9 days.

Equations in Section 4. Water vapor transmission rate (WVTR) and water vapor permeability (WVP) results for all the samples are reported in Figure 4B. PDMS shows a WVTR and WVP values of 180 g $m^{-2}$ $day^{-1}$ and 0.055 g $m^{-1}$ $day^{-1}$ $Pa^{-1}$, respectively, while starch/PDMS materials had a WVTR of 306 g $m^{-2}$ $day^{-1}$ and a WVP of 0.120 g $m^{-1}$ $day^{-1}$ $Pa^{-1}$. This difference can be justified by the introduction in the PDMS's bulk structure of starch granules that probably slightly reduce the barrier properties with respect to the pristine silicone.

WVTR and WVP of PU were 156 g $m^{-2}$ $day^{-1}$ and 0.031 g $m^{-1}$ $day^{-1}$ $Pa^{-1}$, respectively. LWPU samples had values of WVTR and WVP slightly lower with respect to the PU, being 133 g $m^{-2}$ $day^{-1}$ and 0.030 g $m^{-1}$ $day^{-1}$ $Pa^{-1}$, respectively. No significant changes in the barrier properties of the LWPU material with respect to the PU sample were found. This result confirms again that despite the introduction of the lecithin-wax inside the PU, the interactions among the components ensured a well compact bulk structure in the final form, as also noticed in the SEM images in Figure 1E,G, and did not alter the barrier properties of the biocomposite.

Of note that the found WVTR values for the samples under investigation are comparable to that one of common biodegradable plastic such as PLA, PCL, MATER-bi, or polybutylene succinate (PBS).[35]

Finally, the water uptake capacity of the samples was evaluated by placing the materials in a 100% RH chamber for 9 days and their percentage weight gains are reported in Figure 4C. Specifically, a 0.08% of water uptake was observed for the PDMS samples, confirming the well-known hydrophobic behavior of the silicone. Instead, starch/PDMS showed water absorption of 6.90% after 9 days. PU had a value of water uptake of 5.75% while LWPU 7.65%. This outcome suggests an increased hydrophilic nature of this composite with respect to the pristine PU, which was also found in the WCA analysis.

The found differences in wettability, water vapor transmission, and water uptake behavior between the two biocomposites could be the first key for correlating these material features with preferential grown substrates for underwater marine life.

### 2.6. Assessment of Biocomposites Degradation in Marine Environment

Three samples of each biocomposite were placed in the lagoon of Magoodhoo Island between September 2017 and March 2018 to study their degradation underwater. In **Figure 5**A, photographs of the starch/PDMS (up) and LWPU (down) samples underwater at day 0, after 2, 4, and 6 months are shown. As can be noticed, the LWPU biocomposite underwent a faster degradation with respect to the starch-based samples. Indeed, a loss of surface area of 13 ± 2% for starch/PDMS and 45 ± 5% for LWPU samples were calculated. The morphology of the polymeric surface of the two biocomposites was thoroughly altered after the 6 months of immersion, as can be noticed in Figure 5B–E. The starch/PDMS surface was flat and slightly rough before the immersion. Instead, after the immersion period, the surface presented diffused cracks and advanced exfoliation of polymeric pieces, (Figure 5B,C). Similar behavior for PDMS-based materials after immersion in a simulated marine environment for 1 year was also reported by Bele et al.[39] The LWPU samples showed a faster degradation process, and the surface presented big holes/craters where the polymer is being exfoliated, see the red arrows. The thickness of the materials decreased from initial values of 600 ± 50 to 400 ± 20 µm for LWPU and 700 ± 50 to 600 ± 35 µm for starch/PDMS. Therefore there was an average loss of thickness of ≈ 34% and ≈ 15%, respectively for LWPU and starch/PDMS. Weight changes are not reported due to the high quantity of biological material grown on the surface of the two biocomposites, making the weight measurement not accurate. The differences highlighted in the degradation process are

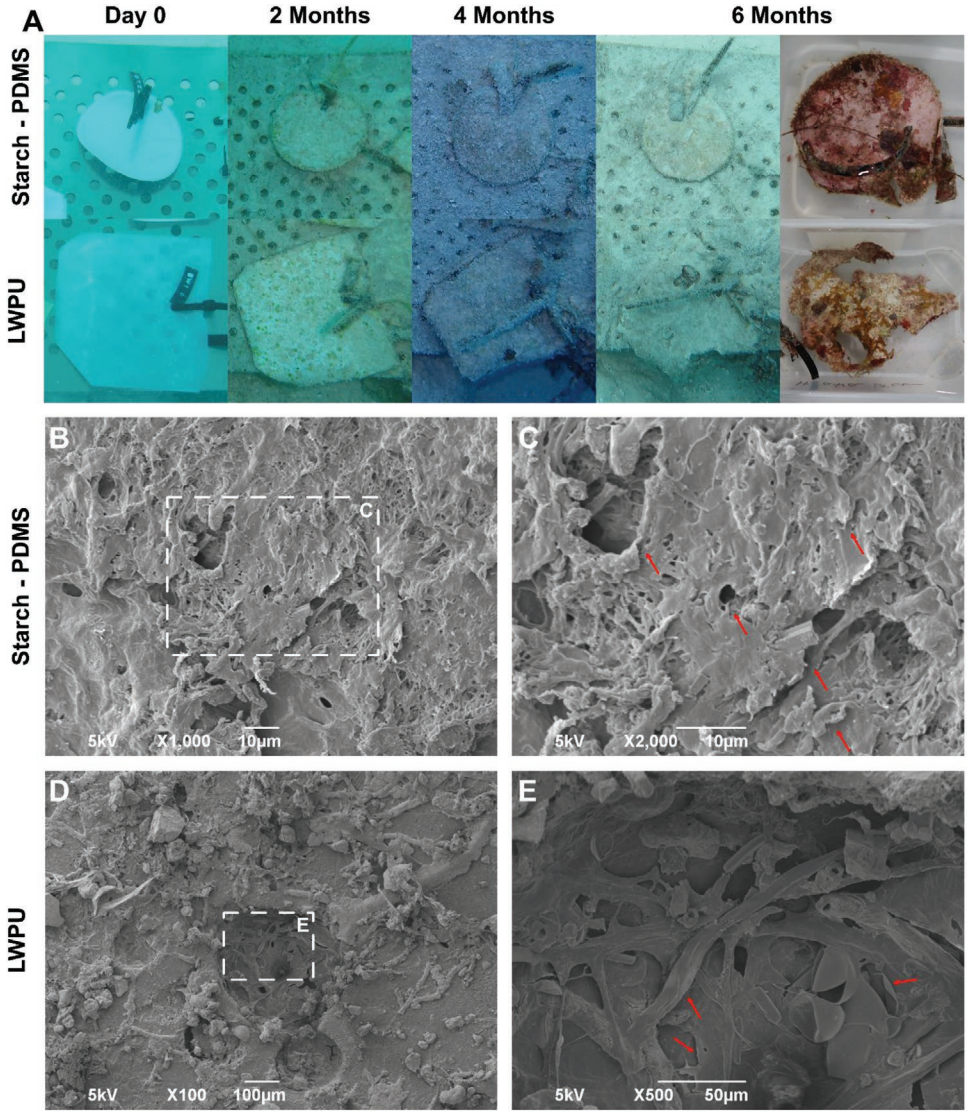


**Figure 5.** A) Underwater and immediately after the immersion period photographs of starch/PDMS (up) and LWPU (down) biocomposites at the different monitoring time points. B,C) SEM images of the starch/PDMS surface after 6 months underwater. The red arrows highlight the holes and the exfoliation process on the surface. D,E) SEM images of the LWPU surface after 6 months underwater. The red arrows highlight the holes and the exfoliation process on the surface.

a consequence of the different nature of the two biocomposites. Indeed, the superficial hydrophobicity of starch/PDMS showed in the WCA analysis drastically slowed down the initial erosion process of the material surface, while the LWPU samples, due to their hydrophilic behavior, are more prone to start the degradation of the materials.

### 2.7. Marine Biodiversity Analysis of Biocomposite Surface

Several biocomposites have already been tested in marine environments,[15,16] but, to the best of our knowledge, this is the first time in a tropical coral reefs ecosystem. After 6 months of underwater deployment, biocomposites were gently taken out from the sea, and their surfaces were analyzed. The material surfaces resulted in being completely changed. Indeed, several organisms both of animal and photosynthetic/vegetable origin colonized the biocomposites. The species and taxonomy level of fouling organisms found on the two biocomposite materials are given in **Table 1**. ≈30 different species belonging to almost 11 phyla were found. For about four specimens, the genus or species was identified, while the remaining (about 80) specimens were not fully identified (Table 1). As seen in Table 1, the Phyla foraminifera, anellida, and ciliophora were the most frequent animal groups found. The highest diversity was apparently discovered in Anellida and Bryozoa with about six species each, whereas the highest number of specimens was discovered in the Phylum ciliophora; an example of this species is reported in Figure S5 in the Supporting Information.

The comparison between the two biocomposites reveals that LWPU appeared more suitable as substrate being colonized by the higher number of phyla, with the presence of coral recruits

**Table 1.** Identification at lower taxonomic level possible and number of specimens for each taxa found on both biocomposites.

| | | | | | | No. of specimens | |
|---|---|---|---|---|---|---|---|
| Phylum | Class | Order | Family | Genus | Species | LWPU | Starch/PDMS |
| Cnidaria | Anthozoa | Scleractinia | | | 3 | 3 | 0 |
| Ctenophora | Tentaculata | Platyctenida | Coeloplanidae | Coeloplana | 1 | 1 | 0 |
| Porifera | | | | | 1 | 0 | 1 |
| Chordata | Ascidiacea | Aplousobranchia | Didemnidae | Polysyncraton | 1 | 0 | 1 |
| Anellida | Polychaeta | Sabellida | Serpulidae | | 6 | 21 | 13 |
| Mollusca | | | | | 2 | 3 | 1 |
| Arthropoda | Hexanauplia | | | | 2 | 4 | 0 |
| | Malacostraca | Amphipoda | | | | | |
| Bryozoa | | | | | 6 | 7 | 1 |
| Foraminifera | | | | | 4 | 12 | 13 |
| Nematoda | | | | | 1 | 1 | 0 |
| Ciliophora | Heterotrichea | Hetereotrichida | Folliculinidae | Halofolliculina | 2 | 33 | 0 |

(**Figure 6**A,B). By contrast, starch/PDMS was colonized by a lower number of phyla, even though some of them as Porifera (sponges) and Chordata (tunicate) appeared to be exclusive of this bio-plastic material (**Figure 7**A,B).

Differences were observed between the two biocomposites also in the coverage of the most common benthic group. In particular, crustose coralline algae (CCA) and sponges covered mainly starch/PDMS compared with LWPU. On the other hand, Bryozoans (Figure 6C,D,G,H) and fleshy algae showed an opposite pattern (**Table 2**). There can be many reasons for these outcomes, with the most likely ones being the large surface area of biocomposites and the presence of a structure that allows fouling organisms to attach themselves to the biocomposites. Even though this is the case, based on the results we obtained, it would be hard to say that fouling organisms make their choice based on the type of biocomposites. However, we may hypothesize that the biodegradation process could increase the roughness or porosity of the material texture, creating a favorable microhabitat for coral larvae colonization. In addition, the different chemical compositions of the two tested biocomposites could play a role in the explanation of the different coral larvae and benthic organisms' settlement. Indeed, PDMS can be degraded in dimethylsilanediol and later in silicic acid.[40] The latter can enter in the silica cycle and affect sediment, benthic fluxes, and potentially enhance sponges grown.[41] In addition, PU could represent a source of nitrogen/ammonium that is reported to be a nutrient to support corals growth.[42] Although it is quite hard to define a correct direction of the reason why we noticed these variations and further studies are required, it appeared evident that the biocomposite named LWPU resulted in being suitable for the settlement of corals, whereas the starch–PDMS not.

Although the number of coral recruits was limited at three, it represents an important insight. Recruitment of new individuals is a critical process for the maintenance and recovery of marine benthic communities.[43] Reef corals may require a sequence of cues for their settlement.[44] These cues are typically associated with or secreted by CCA, microbes in biofilms, or other organisms on the benthos.[45] Since the ecological interactions driving coral recruitment are still poorly understood, especially for those factors that determine successful settlement and metamorphosis, which factors exactly might drive the choice of a specific substrate is actually unknown. Therefore, the development of specific bio-based material able to attract larvae as or even better than a natural substrate can open new perspectives in the conservation strategies aimed to recover the lost coral reef areas.

In addition, it has to be highlighted that coral restoration techniques are based on the use of a large amount of plastic items, mainly represented by cable ties, nylon (fishing net), PVC pipes, and epoxy glue.[46] As such, our results can also open the possibility to design biocomposites that can act as tools for habitat restoration initiatives.

## 3. Conclusions

In this work, we presented the fabrication of two new biocomposites, the first one based on biodegradable polyurethane, wax, and the natural compound soybean lecithin, and produced by water emulsion, while the second one made of starch/PDMS having a weight ratio 60:40 and produced by the solvent casting method. The two biocomposites showed different morphological structures with respect to the pristine siliconic and polyurethane matrices. Interactions among the LWPU sample components were found, suggesting that after the evaporation process, lecithin stabilizes the wax with its hydrophobic part and interacts with PU with its hydrophilic head. The biocomposite resulted in being more ductile with respect to pristine PU, with a reduction of the Young's Modulus and tensile stress. The compact morphological structure and the interactions among the components were also confirmed by similar values found in the WVTR and WVP with respect to the PU, suggesting that despite the change in the structure assembly, the barrier properties were not affected. On the other hand, the introduction of lecithin in the composite led to a slight decrease of the WCA and an increase in the water uptake capacity.

For the starch/PDMS sample, an increase of YM and tensile stress and a reduction of elongation were described. These

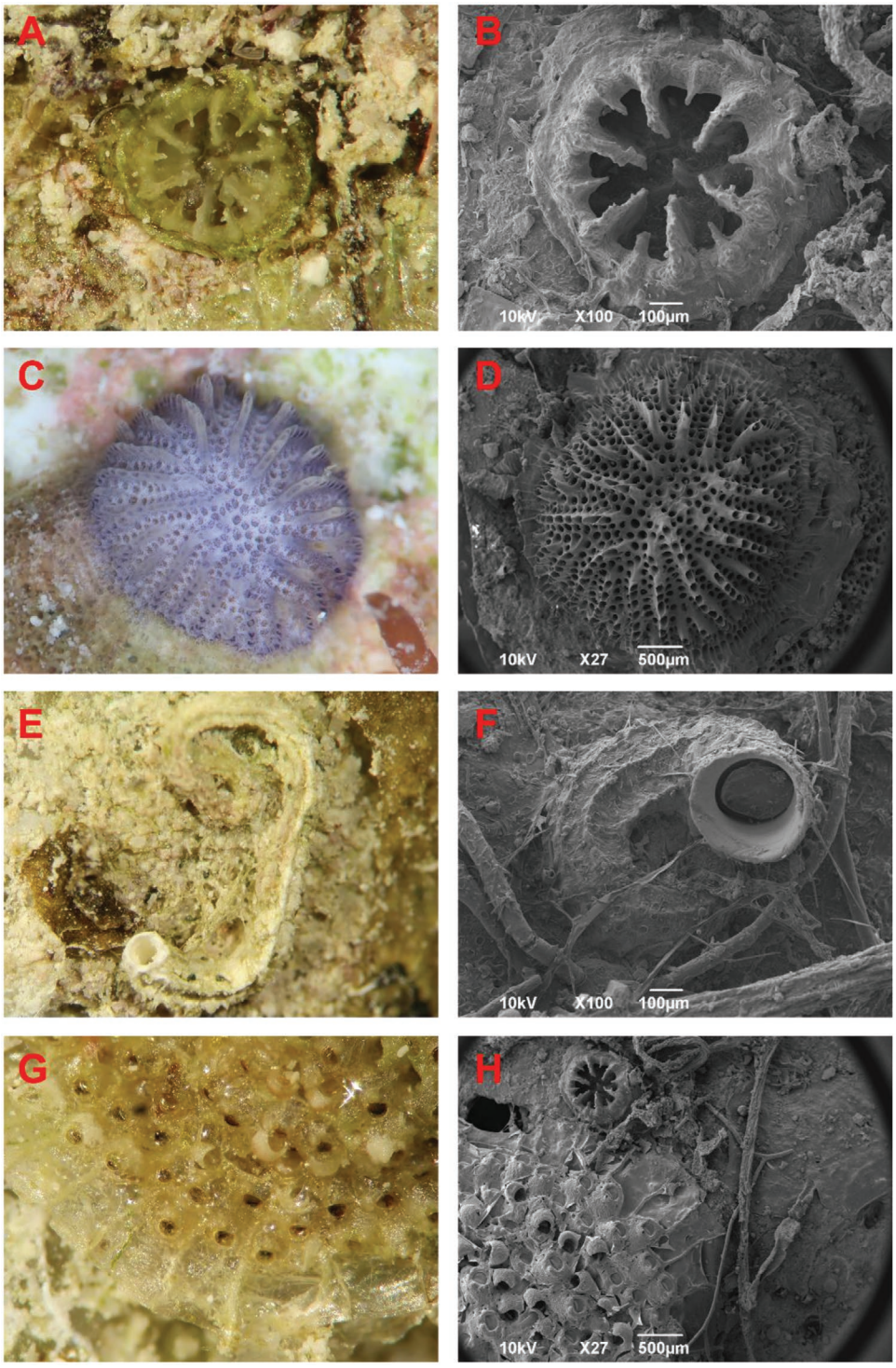


**Figure 6.** A,B) Live and SEM images of coral recruits, respectively, on LWPU samples surface. C,D) Live and SEM images of a bryozoan, respectively, on LWPU samples surface. E,F) Live and SEM images of two different serpulid polychaetes, respectively, on LWPU samples surface. G,H) Live and SEM images of another bryozoan species, respectively, on LWPU samples surface.

outcomes were in agreement with the mechanical properties found by using DMA in our previous work. After 6 months of immersion in the Maldivian Sea, both the biocomposites began to degrade and the LWPU lost around 45% of their initial area.

As a first study conducted on the coral reef ecosystem evaluating the growth of benthic fouling organisms on biocomposites, our observations indicated that there were significant amounts of organisms able to settle on these biocomposite films in a Maldivian lagoon, both of animal and photosynthetic

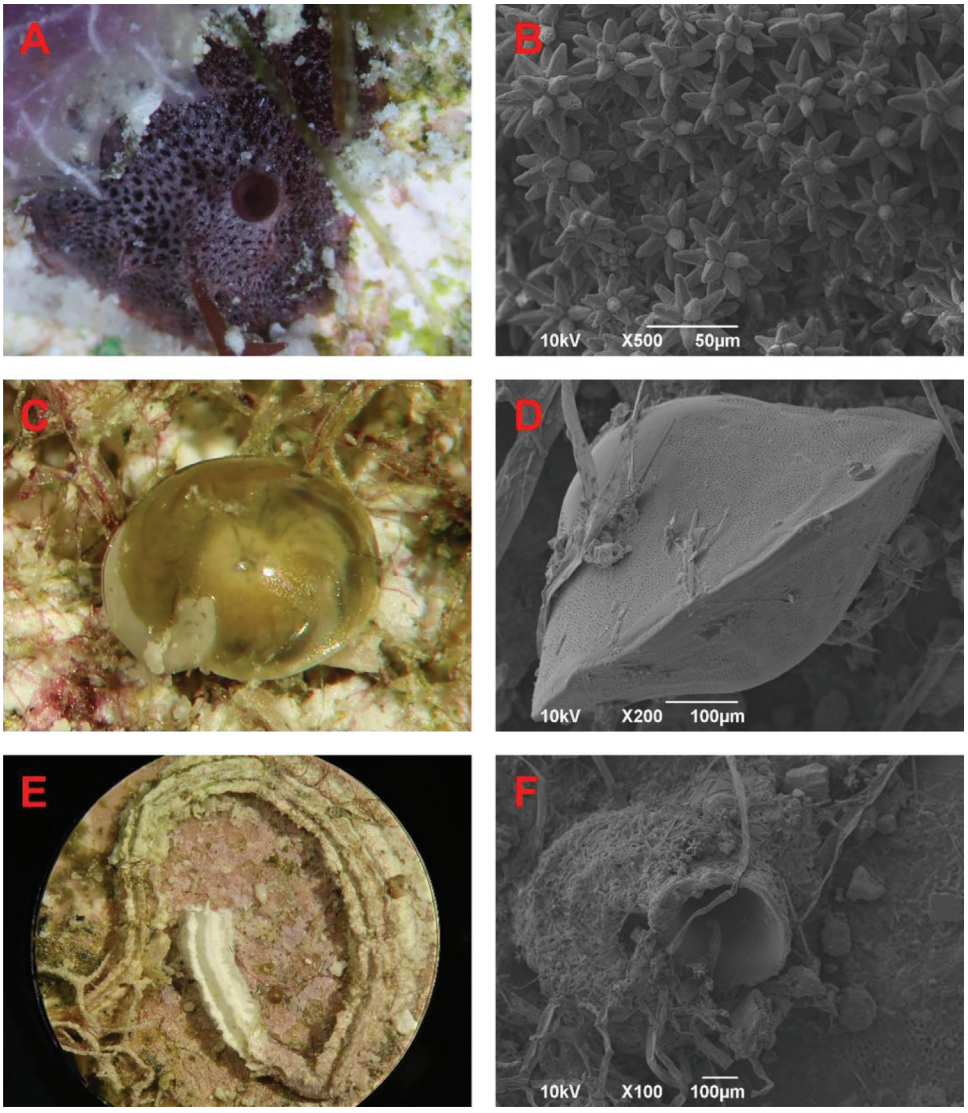


**Figure 7.** A,B) Live and SEM images of *Polysyncraton* sp. (Chordata) and its spicules, respectively, on starch/PDMS samples surface. C,D) Live and SEM images of a foraminifera, respectively, on starch/PDMS samples surface. E,F) Live and SEM images of two different serpulid polychaetes, respectively, on starch/PDMS samples surface.

nature, suggesting that biocomposites have the potentiality to become a suitable substrate for many other hard bottom fouling organisms. Moreover, significant differences with regards to the diversity and abundance of species that colonized the two biocomposites were found. Finally, the presence of several coral larvae on LWPU sample strongly indicates that this kind of biocomposites could provide a double benefit to the marine environment, reducing the impacts related to environmental changes and pollution, and creating a new, technologically advanced, artificial substrate to help the recovery of an ecosystem, such as coral reefs, on the verge of death.

**Table 2.** Coverage (%) of the main taxa between the two biocomposites.

| | LWPU | Starch/PDMS |
|---|---|---|
| Crustose coralline algae | 16.88 ± 1.48 | 59.15 ± 3.40 |
| Sponges | nd | 6.05 ± 1.96 |
| Chordata | nd | 1.56 ± 1.45 |
| Serpulids | 4.27 ± 0.72 | 3.88 ± 2.82 |
| Bryozoans | 6.38 ± 1.24 | nd |
| Fleshy algae | 27.2 ± 4.33 | 25.23 ± 2.14 |
| Bare material/sediment | 40.09 ± 4.50 | nd |
| Unknown | 6.29 ± 0.48 | 4.33 ± 0.48 |

## 4. Experimental Section

*Materials*: Unmodified regular corn starch containing ≈73% amylopectin and 27% amylose, reagent grade heptane, and paraffin wax were purchased from Sigma Aldrich and used as received. Acetoxypolysiloxane (Acetoxy-PDMS; Elastosil E43) was purchased from Wacker Chemie AG and used as received. This product is a one-component mixture of hydroxyl end-blocked polydimethylsiloxane, also

known as hydroxylterminated PDMS, and triacetoxy(methyl)-silane (<10%) using dibutyltin diacetate (<0.1%) as a catalyst. As a source of biodegradable PU, a polycaprolactone diol based water-suspension known as Aquaréthane (Syntilor, France) developed as biobased wood coating was used. The aqueous suspension did not contain any other additives or pigments. Granules of soybeans lecithin were obtained from Lecinova (Italy), a food integrator commercialized by Céréal.

*Preparation of the Biocomposites*: Starch-based biocomposites were produced as followed: 6 g of elastosil E43 were weighed and gently mixed with 15 mL of heptane, then 9 g of corn starch was added to the solution and mixed until all the clusters were dispersed. Afterward, the mix was placed in a glass Petri dish and dried under an aspirated hood at ambient conditions (16–20 °C and 40–50% RH) for 4 days. Composites with a starch/PDMS weight ratio of 60:40 were obtained.

A second biocomposite was produced by emulsifying paraffin wax in the water-based polyurethane solution using soybeans lecithin. Specifically, 0.75 g of lecithin was added to 24 mL of water and mixed by using a Sonics Vibra-Cell ultrasonicator for 1 min and 30 s with 40% amplitude for three times to obtain a complete dissolution of the compound while the solution becomes slightly orange. 1.5 g of wax was added to the mix and they were warmed at 80 °C by using a hot gun until all the wax was melted. Immediately after, the mix underwent a second round of ultrasonicator again for 1 min and 30 s with 40% amplitude for three times, until the solution got a milky color. 12 mL of emulsion was mixed with 12 mL of an aqueous PU suspension (33% w/v) (emulsion/PU volume ratio 1:1), and four other sonication steps (1:30 min) were performed to stabilize the final emulsion. The mix was placed in a plastic Petri dish and let to dry for 4 days at ambient conditions (16–20 °C and 40–50% RH). A schematic representation of the LWPU sample preparation is shown in Scheme 1. Note that on a daily basis the composite film contained 64 wt% PU, 12 wt% soy lecithin, and 24 wt% wax. The produced biocomposites were named starch–PDMS and LWPU, respectively. Control films of pristine silicone and polyurethane were also produced and labeled as PDMS and PU, respectively.

*Morphological Analysis*: The morphology of the obtained biocomposites was analyzed by SEM, using a variable pressure JOEL JSM-649LA microscope equipped with a tungsten thermionic electron source and working in a high vacuum mode, with an acceleration voltage of 5 and 10 kV. The specimens were coated with a 10 nm thick film of gold using a Cressington Sputter Coater-208 HR.

*ATR–FTIR*: Infrared spectra of the biocomposites materials were acquired by using an ATR accessory (MIRacle ATR, PIKE Technologies) with a diamond crystal coupled to an FTIR spectrometer (Vertex 70v FT-IR, Bruker). All spectra were recorded in the range between 4000 and 600 $cm^{-1}$, with a resolution of 4 $cm^{-1}$, accumulating 128 scans. For the subtraction of spectra, they were previously normalized to the band of C=O stretching mode at 1728 $cm^{-1}$ of PU.

*X-ray Diffraction*: The physical state of the final biocomposites and their pristine components was determined by X-ray diffraction spectroscopy. In particular, X-ray diffractograms were obtained by using a PANalytical Empyrean X-ray diffractometer equipped with a 1.8 kW Cu K$\alpha$ source sealed in a ceramic tube, and a 0D Xe proportional detector with Pixcel3D2×2 area detector. The samples were placed on a quartz support and experiments were performed using Cu K$\alpha$ anode ($\lambda = 1.5406$ A) operated at 45 kV and 40 mA from 5° to 65° 2$\theta$.

*Thermal Characterization*: The thermal degradation behavior of the biocomposites and their pristine components was determined by thermogravimetric analysis (TGA) and using a TGA Q500 from TA Instruments. Measurements were carried out using 3–5 mg of sample in an aluminum pan under inert $N_2$ flow (50 mL $min^{-1}$) in a temperature range from 30 to 800 °C and with a heating rate of 5 °C $min^{-1}$. The weight loss and its first derivative were acquired simultaneously as a function of time/temperature.

*Mechanical Characterization*: The mechanical properties of LWPU, starch/PDMS, PU, and PDMS samples were determined by uniaxial tension tests on a dual column universal testing machine (Instron 3365). Biocomposites were cut in dog bone specimens (at least seven of them for each sample) with a width of 4 mm and an adequate length of 25 mm. Displacement was applied at a rate of 10 mm $min^{-1}$. The Young's Modulus, stress at maximum load, and elongation at break were calculated from the stress–strain curves. All the stress–strain curves were recorded at 25 °C and 44% RH.

*Water Contact Angles*: Static water contact angle analysis was performed by using the sessile drop method with a DataPhysics OCAH 200 contact angle goniometer equipped with a CCD camera and image processing software operating under laboratory conditions (temperature 22–25 °C and relative humidity 50–60%). For the characterization, droplets of 1 mL volume MilliQ water were used. Up to 15 contact angle measurements were carried out on each sample at random locations, and their average values and standard deviation were reported.[47]

*Water Vapor Permeability*: WVP of the films was determined at 25 °C and under 100% RH according to the ASTM E96 standard method. 100% RH was reached by placing 400 µL of deionized water in the permeation chambers of 7 mm inner diameter and 10 mm inner depth.

The samples were cut, placed on the top of the permeation chamber, and sealed through O-rings and screws. The chambers were placed in a desiccator and maintained at 0% RH by anhydrous silica gel.

The weight changes of the chambers were collected every hour for eight consecutive hours, in order to monitor the transfer of water from the chamber, through the sample, to the silica gel. An electronic balance (0.0001 g accuracy) was used to record mass loss over time. The water mass loss of permeation chambers was plotted as a function of time. The slope of each line was calculated by linear regression. Then, the WVTR was determined as below

$$\mathrm{WVTR}\left(g\left(m^2 d\right)^{-1}\right) = \frac{\text{slope}}{\text{area of the sample}} \tag{1}$$

The WVP of the samples was calculated as follows

$$\mathrm{WVP}\left(g\left(md\ \mathrm{Pa}\right)^{-1}\right) = \frac{\mathrm{WVTR}\cdot L\cdot 100}{p_s\cdot \Delta \mathrm{RH}} \tag{2}$$

where $L$ (m) is the thickness of the sample, which was measured with a micrometer with 0.001 mm accuracy, ΔRH (%) is the percentage relative humidity gradient, and $p_s$ (Pa) is the saturation water vapor pressure at the experimental temperature of 25 °C.[36] Every measurement was replicated three times.

*Water Uptake*: Water uptake measurements on films were also performed. Samples were first placed in a dry chamber with anhydrous silica gel desiccant for 24 h. Dehydrated samples were weighed on a sensitive electronic balance (0.0001 g accuracy) and then sealed in a humidity chamber at 100% RH. Samples were kept in the humidity chamber for several days, during which they were weighed every 24 h. The amount of adsorbed water was calculated based on the initial dry weight as the difference, according to the following formula

$$\text{water adsorption } (\%) = \frac{m_f - m_0}{m_0}\cdot 100 \tag{3}$$

where $m_f$ is the sample weight at 100% RH condition and $m_0$ is the sample at 0% RH. The test proceeded until stabilization of weight gain that is when the sample adsorbed water gets in equilibrium with the 100% humid environment.[47] Every sample was analyzed five times.

*Marine Biodiversity Study*: The study was conducted during September 2017 and March 2018 in Faafu Atoll, Republic of Maldives (Figure S1, Supporting Information). This atoll is ≈31 km long and 24 km wide and is subjected to two main oceanic stream/currents: one toward southwest–northeast from May to November, and another in the opposite direction from December to April.[48] Operations were carried out by using the Marine Research and High Education Center (MaRHE) as a logistic station and marine laboratories facility. This center is placed on Magoodhoo Island (3°4′49.08″N, 72°57′57.19″E), a scarcely inhabited island (≈850 people) that measures 900 × 450 m and is located on the southeast part of the atoll rim (Figure S1, Supporting Information).

Six samples of biocomposites were weighed and then deployed on a flat support 35 cm above the sandy bottom in a sheltered lagoon of Magoodhoo at 8 m depth. Each of them were tagged and monitored "monthly"–"weekly" in order to check the material status for a total of 6 months. Qualitative information of presence/absence of algae, CCA, predator scars, corals, and "others" was gathered in each survey. The presence and absence of seastar, mollusk, bryozoans, ascidians, hydrozoans, sponges, and the remaining are referred as the category other. For each sample, at the end of the monitoring period, 15 × 15 cm photos were collected to assess the coverage of the organisms that colonized the bio-material. Photographs were taken during sampling activities using a Canon G11 camera in an underwater housing Canon WP-DC 34, and the photographs were analyzed using Coral Point Count with Excel extension software (CPCe 4.1).

Finally, in order to identify and count the organisms found on different biocomposites, each sample was carefully observed under a Leica EZ4 D stereomicroscope. Furthermore, to determine the lowest possible taxonomic level at which the organisms were found, several additional SEM analyses were performed. For the SEM analyses, the materials were sputter-coated with gold and observed using the same procedure and equipment described in Section 2.3.

## Supporting Information

Supporting Information is available from the Wiley Online Library or from the author.

## Acknowledgements

M.C. and S.M. contributed equally to this work.

## Conflict of Interest

The authors declare no conflict of interest.

## Data Availability Statement

Research data are not shared.

## Keywords

biocomposites, biodegradable materials, coral restoration

Received: March 23, 2021
Revised: June 25, 2021
Published online:

[1] a) T. P. Hughes, K. D. Anderson, S. R. Connolly, S. F. Heron, J. T. Kerry, J. M. Lough, A. H. Baird, J. K. Baum, M. L. Berumen, T. C. Bridge, *Science* **2018**, *359*, 80; b) T. P. Hughes, M. L. Barnes, D. R. Bellwood, J. E. Cinner, G. S. Cumming, J. B. Jackson, J. Kleypas, I. A. Van De Leemput, J. M. Lough, T. H. Morrison, *Nature* **2017**, *546*, 82; c) A. R. Harborne, A. Rogers, Y.-M. Bozec, P. J. Mumby, **2017**, *9*, 445.

[2] F. Saliu, S. Montano, B. Leoni, M. Lasagni, P. Galli, *Mar. Pollut. Bull.* **2019**, *142*, 234.

[3] M. de Oliveira Soares, E. Matos, C. Lucas, L. Rizzo, L. Allcock, S. Rossi, *Mar. Pollut. Bull.* **2020**, *161*, 111810.

[4] J. B. Lamb, B. L. Willis, E. A. Fiorenza, C. S. Couch, R. Howard, D. N. Rader, J. D. True, L. A. Kelly, A. Ahmad, J. Jompa, *Science* **2018**, *359*, 460.

[5] R. Costanza, R. De Groot, P. Sutton, S. Van der Ploeg, S. J. Anderson, I. Kubiszewski, S. Farber, R. K. Turner, *Global Environ. Change* **2014**, *26*, 152.

[6] a) L. Boström-Einarsson, R. C. Babcock, E. Bayraktarov, D. Ceccarelli, N. Cook, S. C. Ferse, B. Hancock, P. Harrison, M. Hein, E. Shaver, *PLoS One* **2020**, *15*, e0226631; b) M. Contardi, S. Montano, G. Liguori, J. A. Heredia-Guerrero, P. Galli, A. Athanassiou, I. S. Bayer, *Sci. Rep.* **2020**, *10*, 988.

[7] a) P. Singh, R. Verma, in *Environmental Microbiology and Biotechnology*, Springer, Berlin **2020**, p. 35; b) S. RameshKumar, P. Shaiju, K. E. O'Connor, *Curr. Opin. Green Sustainable Chem.* **2020**, *21*, 75; c) A. K. Mohanty, S. Vivekanandhan, J.-M. Pin, M. Misra, *Science* **2018**, *362*, 536; d) I. D. Posen, P. Jaramillo, A. E. Landis, W. M. Griffin, *Environ. Res. Lett.* **2017**, *12*, 034024.

[8] a) G. Lligadas, J. C. Ronda, M. Galià, V. Cádiz, *Polymers* **2010**, *2*, 440; b) A. Zych, J. Tellers, L. Bertolacci, L. Ceseracciu, L. Marini, G. Mancini, A. Athanassiou, *ACS Appl. Polym. Mater.* **2021**, *3*, 1135; c) U. Biermann, U. Bornscheuer, M. A. Meier, J. O. Metzger, H. J. Schäfer, *Angew. Chem., Int. Ed.* **2011**, *50*, 3854.

[9] a) B. Khan, M. Bilal Khan Niazi, G. Samin, Z. Jahan, *J. Food Process Eng.* **2017**, *40*, e12447; b) K. W. Meereboer, M. Misra, A. K. Mohanty, *Green Chem.* **2020**, *22*, 5519; c) M. Yamada, S. Morimitsu, E. Hosono, T. Yamada, *Int. J. Biol. Macromol.* **2020**, *149*, 1077.

[10] a) G. Perotto, L. Ceseracciu, R. Simonutti, U. C. Paul, S. Guzman-Puyol, T.-N. Tran, I. S. Bayer, A. Athanassiou, *Green Chem.* **2018**, *20*, 894; b) J. X. Chan, J. F. Wong, A. Hassan, Z. Zakaria, in *Biopolymers and Biocomposites from Agro-Waste for Packaging Applications*, Elsevier, Amsterdam **2021**, p. 141; c) I. S. Bayer, S. Guzman-Puyol, J. A. Heredia-Guerrero, L. Ceseracciu, F. Pignatelli, R. Ruffilli, R. Cingolani, A. Athanassiou, *Macromolecules* **2014**, *47*, 5135.

[11] N. Mahajan, P. Gupta, *RSC Adv.* **2015**, *5*, 41839.

[12] a) Y. Akutsu-Shigeno, Y. Adachi, C. Yamada, K. Toyoshima, N. Nomura, H. Uchiyama, T. Nakajima-Kambe, *Appl. Microbiol. Biotechnol.* **2006**, *70*, 422; b) A. Loredo-Treviño, G. Gutiérrez-Sánchez, R. Rodríguez-Herrera, C. N. Aguilar, *J. Polym. Environ.* **2012**, *20*, 258.

[13] a) R. A. Wilkes, L. Aristilde, *J. Appl. Microbiol.* **2017**, *123*, 582; b) C. Ruiz, T. Main, N. P. Hilliard, G. T. Howard, *Int. Biodeterior. Biodegrad.* **1999**, *43*, 43.

[14] a) J. R. Russell, J. Huang, P. Anand, K. Kucera, A. G. Sandoval, K. W. Dantzler, D. Hickman, J. Jee, F. M. Kimovec, D. Koppstein, *Appl. Environ. Microbiol.* **2011**, *77*, 6076; b) L. Cosgrove, P. L. McGeechan, G. D. Robson, P. S. Handley, *Appl. Environ. Microbiol.* **2007**, *73*, 5817.

[15] P. Davies, G. Evrard, *Polym. Degrad. Stab.* **2007**, *92*, 1455.

[16] M. Rutkowska, K. Krasowska, A. Heimowska, I. Steinka, H. Janik, *Polym. Degrad. Stab.* **2002**, *76*, 233.

[17] E. Wondu, H. W. Oh, J. Kim, *Polymers* **2019**, *11*, 1915.

[18] E. Ayres, R. L. Oréfice, M. I. Yoshida, *Eur. Polym. J.* **2007**, *43*, 3510.

[19] S.-h. Hsu, L.-G. Dai, Y.-M. Hung, N.-T. Dai, *Int. J. Nanomed.* **2018**, *13*, 5485.

[20] Z. Yang, G. Wu, *J. Mater. Sci.* **2020**, *55*, 3139.

[21] a) R. Lehmann, S. Varaprath, C. Frye, *Environ. Toxicol. Chem.* **1994**, *13*, 1753; b) R. Lehmann, S. Varaprath, C. Frye, *Environ. Toxicol. Chem.* **1994**, *13*, 1061; c) R. G. Lehmann, J. R. Miller, *Environ. Toxicol. Chem.* **1996**, *15*, 1455.

[22] J. Spivack, S. B. Dorn, *Environ. Sci. Technol.* **1994**, *28*, 2345.

[23] C. Sabourin, J. Carpenter, T. Leib, J. Spivack, *Appl. Environ. Microbiol.* **1996**, *62*, 4352.

[24] a) L. Ceseracciu, J. A. Heredia-Guerrero, S. Dante, A. Athanassiou, I. S. Bayer, *ACS Appl. Mater. Interfaces* **2015**, *7*, 3742; b) T. N. Tran, A. Athanassiou, A. Basit, I. S. Bayer, *Food Chem.* **2017**, *216*, 324; c) T. N. Tran, J. A. Heredia-Guerrero, B. T. Mai, L. Ceseracciu,

L. Marini, A. Athanassiou, I. S. Bayer, *Adv. Sustainable Syst.* **2017**, *1*, 1700002.
[25] F. Razza, F. Degli Innocenti, A. Dobon, C. Aliaga, C. Sanchez, M. Hortal, *J. Cleaner Prod.* **2015**, *102*, 493.
[26] S. Derkach, T. Dyakina, S. Levachev, *Colloid J.* **2005**, *67*, 547.
[27] G. Trovati, E. A. Sanches, S. C. Neto, Y. P. Mascarenhas, G. O. Chierice, *J. Appl. Polym. Sci.* **2010**, *115*, 263.
[28] X. Wang, Z. Luo, Z. Xiao, *Carbohydr. Polym.* **2014**, *101*, 1027.
[29] W. Chen, Z. Zhao, C. Yin, *Fuel* **2010**, *89*, 1127.
[30] A. Lopez-Rubio, B. M. Flanagan, E. P. Gilbert, M. J. Gidley, *Biopolymers* **2008**, *89*, 761.
[31] D. Merino, R. Ollier, M. Lanfranconi, V. Alvarez, *Appl. Clay Sci.* **2016**, *127*, 17.
[32] M. Mochane, A. Luyt, *Thermochim. Acta* **2012**, *544*, 63.
[33] Y. Tian, Y. Li, X. Xu, Z. Jin, *Carbohydr. Polym.* **2011**, *84*, 1165.
[34] G. Robertson, in *Environmentally Compatible Food Packaging*, Elsevier, Amsterdam **2008**, p. 3.
[35] G. Scoponi, S. Guzman-Puyol, G. Caputo, L. Ceseracciu, A. Athanassiou, J. A. Heredia-Guerrero, *Polymer* **2020**, *193*, 122371.
[36] J. A. Heredia-Guerrero, J. J. Benítez, P. Cataldi, U. C. Paul, M. Contardi, R. Cingolani, I. S. Bayer, A. Heredia, A. Athanassiou, *Adv. Sustainable Syst.* **2017**, *1*, 1600024.
[37] K. E. Borchani, C. Carrot, M. Jaziri, *Composites, Part A* **2015**, *78*, 371.
[38] R. Nirmala, H.-M. Park, R. Navamathavan, H.-S. Kang, M. H. El-Newehy, H. Y. Kim, *Mater. Sci. Eng., C* **2011**, *31*, 486.
[39] A. Bele, G. Stiubianu, S. Vlad, C. Tugui, C. Varganici, L. Matricala, D. Ionita, D. Timpu, M. Cazacu, *RSC Adv.* **2016**, *6*, 8941.
[40] C. Stevens, *J. Inorg. Biochem.* **1998**, *69*, 203.
[41] P. J. Tréguer, C. L. De La, Rocha, *Annu. Rev. Mar. Sci.* **2013**, *5*, 477.
[42] N. Rädecker, C. Pogoreutz, C. R. Voolstra, J. Wiedenmann, C. Wild, *Trends Microbiol.* **2015**, *23*, 490.
[43] a) A. Underwood, P. Fairweather, *Trends Ecol. Evol.* **1989**, *4*, 16; b) S. Gaines, J. Roughgarden, *Proc. Natl. Acad. Sci. USA* **1985**, *82*, 3707.
[44] P. T. Raimondi, A. N. Morse, *Ecology* **2000**, *81*, 3193.
[45] a) P. Ettinger-Epstein, S. Whalan, C. N. Battershill, R. de Nys, *Mar. Ecol. Prog. Ser.* **2008**, *365*, 103; b) M. G. Hadfield, *Annu. Rev. Mar. Sci.* **2011**, *3*, 453; c) L. Harrington, K. Fabricius, G. De'Ath, A. Negri, *Ecology* **2004**, *85*, 3428; d) A. Heyward, A. Negri, *Coral Reefs* **1999**, *18*, 273.
[46] S. Frias-Torres, P. Montoya-Maya, N. Shah, *Coral Reef Restoration Toolkit: A Field-Oriented Guide Developed in the Seychelles Islands* **2019**, https://doi.org/10.31230/osf.io/8eua9.
[47] G. Mazzon, M. Contardi, A. Quilez-Molina, M. Zahid, E. Zendri, A. Athanassiou, I. S. Bayer, *Colloids Surf. A* **2020**, *613*, 126061.
[48] S. Montano, G. Strona, D. Seveso, P. Galli, *Diseases of Aquatic Organisms* **2012**, *101*, 159.